

This is post-print version of the paper published in:
***J. Phys. D: Appl. Phys.* 49 (2016); 435106 - 435112**
DOI: [10.1088/0022-3727/49/43/435106](https://doi.org/10.1088/0022-3727/49/43/435106)

The composition effect on the thermal and optical properties across CdZnTe crystals

K. Strzalkowski

Institute of Physics, Faculty of Physics, Astronomy and Informatics, Nicolaus Copernicus University, Grudziadzka 5, 87-100 Torun, Poland
skaroll@fizyka.umk.pl

Abstract

Cd_{1-x}Zn_xTe mixed crystals investigated in this work were grown from the melt by vertical Bridgman-Stockbarger method in the whole range of composition $0 < x < 1$ that is from one binary crystal (CdTe) to another (ZnTe). The real composition of grown crystals was measured with SEM/EDS method along growth axis. The segregation coefficient of Zn in CdTe matrix has been evaluated as close to unity. The energy gap as a function of the composition was determined from transmission spectroscopy. Thanks to that bowing parameter of this ternary alloy was found to be 0.458. In this work for the first time the systematical study of thermal properties of Cd_{1-x}Zn_xTe alloys from one binary crystal (CdTe) to another (ZnTe) grown by vertical Bridgman technique were undertaken. The thermal diffusivity and effusivity of investigated crystals were derived from the experimental data and allowed calculating the thermal conductivity. Diagrams of the thermal conductivity versus composition were analyzed applying model for mixed semiconducting crystals given by Sadao Adachi. Thanks to that contribution of the thermal resistivity arising from the lattice disorder to the total resistivity of the crystal has been determined.

Keywords: Semiconductors alloys; Crystal growth; Segregation coefficient; Bowing parameter; Thermal conductivity; CdZnTe crystals

1 Introduction

CdTe and $\text{Cd}_{1-x}\text{Zn}_x\text{Te}$ in bulk crystal form have a fairly long history and are used in a variety of applications as x-ray and gamma-ray detectors [1-4], in electrooptic and photorefractive devices [5] and as substrates for epitaxy in case of infrared detectors [6]. In last twenty years $\text{Cd}_{1-x}\text{Zn}_x\text{Te}$ crystals for composition of the order of 10 to 20 atomic percentages have become one of the most studied materials for gamma-ray detection application and also spectroscopic x-ray imaging [7]. The variation in composition allows tuning of their fundamental parameters like energy band-gap and lattice constant, what is very important from the application point of view. For this reason one of the goal of this work is evaluating bowing parameter for $\text{Cd}_{1-x}\text{Zn}_x\text{Te}$ mixed crystals grown with modified Bridgman technique.

Nowadays one can get commercially available large, high-quality $\text{Cd}_{1-x}\text{Zn}_x\text{Te}$ crystals [8] and many kinds of x-ray and gamma-ray detectors manufactured from them. The unique properties of $\text{Cd}_{1-x}\text{Zn}_x\text{Te}$ at room temperature make it an ideal detector solution for Medical, Industrial, Homeland Security and Laboratory applications [1]. CdTe based mixed crystals meet several critical requirements for gamma-ray detection. Both, cadmium and telluride possess high atomic numbers (Z). The cross-section for photoelectric absorption in a material strongly depends on its atomic number (Z^n , where $4 < n < 5$). The energy bandgap of CdTe based compounds is large enough (>1.5 eV) for high resistivity and low leakage current, but on the other hand is small enough (< 5 eV) so that the electron-hole ionization energy is small. However, there are still some shortcomings which should be considered. The main reason why growing of large and homogenous crystals is still problematic is non-unity segregation coefficient of zinc in CdTe matrix (1.35 [9]). Therefore another goal of the work is to verify the segregation coefficient along growth axis of grown $\text{Cd}_{1-x}\text{Zn}_x\text{Te}$ crystals for different composition.

The key property of materials used for detecting application is their quality [10]. Since efficiency and sensitivity of the potential detector strongly depends on the quality of used crystal it is of high importance to define its lattice disorder. It was shown how lattice disorder effects in case of $\text{Zn}_{1-x}\text{Be}_x\text{Se}$ and $\text{Zn}_{1-x}\text{Mg}_x\text{Se}$ crystals affect physical properties of mixed compounds [11]. However, due to instability at higher concentration, measurements for given semiconductors were carried out in the range of composition from $x = 0$ to $x = 0.5$. The aim of this work is to trace the changes of thermal parameters from one binary compound to another one in whole change of x (from CdTe to ZnTe). To achieve this goal, photopyroelectric technique in both, back (BPPE) and front (FPPE) configuration will be applied for thermal inspection of the samples [12]. Thermal diffusivity, effusivity and conductivity are interrelated with simple dependencies, so the thermal conductivity of investigated materials can be calculated. The composition effect on thermal properties of given crystals will be presented and discussed. Obtained results will be analyzed in theoretical model given by Sadao Adachi for mixed crystals [13].

2 Experimental set up and sample preparation

2.1 Samples description

Investigated in this work $\text{Cd}_{1-x}\text{Zn}_x\text{Te}$ crystals were grown by the high temperature and high pressure vertical Bridgman-Stockbarger method with different Cd and Zn content. Several $\text{Cd}_{1-x}\text{Zn}_x\text{Te}$ crystals with following zinc content (x) were grown: 0 (CdTe), 0.05, 0.1, 0.5, 0.9, 0.95 and 1 (ZnTe). To prevent the evaporation during the crystal growth process an argon overpressure of about 150 atm. was applied. Pure binary powders of CdTe and ZnTe (6N, Koch-Light) mixed together in stoichiometric proportion were put into graphite crucible and kept at temperature of about 1650 K for a few hours and then moved out from the heating zone at a speed of 2.4 mm/h. More details concerning technical data of this process were published elsewhere [14]. Grown in this way crystal rods were of 1 cm in diameter and up to few cm in length. Obtained ingots were cut with wire saw perpendicular to the growth axis into about 1-1.5 mm slices, which were not orientated along any crystallographic plane. The plates were first mechanically ground (Al_2O_3 powder, 10 μm) and then polished with diamond paste (0.1-1 μm). Such prepared specimens were investigated in this work. The real contents of Cd, Zn and Te in this ternary alloy were determined with the SEM/EDS method. Quantax 200 X-ray spectrometer and EDX XFlash 4010 detector with 20 keV excitation energy were used in order to acquire characteristic radiation. Fig. 1 presents example EDX spectra of $\text{Cd}_{1-x}\text{Zn}_x\text{Te}$ crystals under 20 keV excitation.

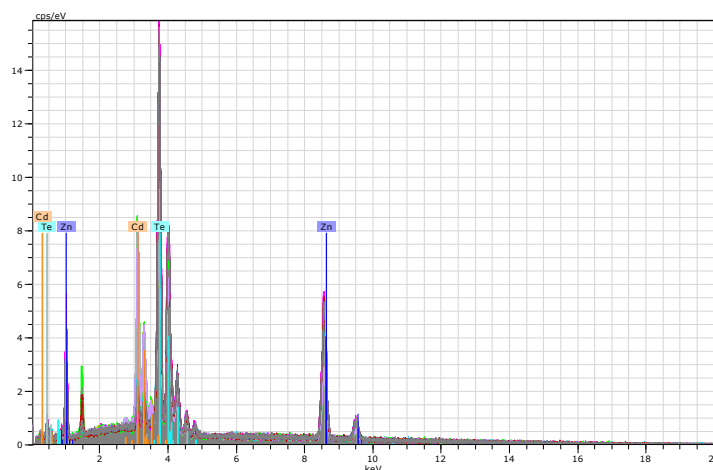


Fig. 1 Example EDX spectra of $\text{Cd}_{1-x}\text{Zn}_x\text{Te}$ crystals under 20 keV excitation.

From one grown boule one can obtain up to 15 plates, depending on their thickness and length of given rod (see Fig. 2).

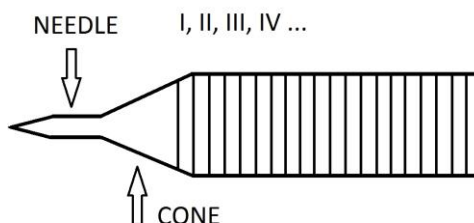


Fig. 2 Cutting scheme of grown crystal rods.

The real composition of grown crystals was determined every third plate for all $\text{Cd}_{1-x}\text{Zn}_x\text{Te}$ alloys. For each sample the analysis was done at three different places on the surface of area of about 0.1×0.1 mm. Therefore obtained results presented in Table 1 are average values with standard deviation and are given in atomic percent of zinc content in $\text{Cd}_{1-x}\text{Zn}_x\text{Te}$ crystals.

Table 1 The composition of $\text{Cd}_{1-x}\text{Zn}_x\text{Te}$ alloys along grown crystal rods.

%	I	IV	VII	X	XIII	XIV	XV
5	-	7.03 ± 0.28	6.88 ± 0.29	6.98 ± 0.30	6.53 ± 0.19	-	-
10	11.06 ± 0.33	11.07 ± 0.15	11.11 ± 0.52	-	11.30 ± 0.28	-	9.98 ± 0.16
50	54.11 ± 0.79	50.30 ± 0.85	47.86 ± 1.62	49.00 ± 0.29	47.90 ± 0.85	-	-
90	91.45 ± 0.37	90.80 ± 0.29	89.81 ± 0.26	89.07 ± 0.63	88.44 ± 0.30	-	-
95	95.84 ± 0.11	95.19 ± 0.13	94.87 ± 0.09	94.25 ± 0.48	93.53 ± 0.44	91.50 ± 0.47	-

An inspection of results presented in Table 1 lead to conclusion that zinc content along growth axis does not change much for all crystals and as the consequence the segregation coefficient of zinc in CdTe matrix should be close to unity.

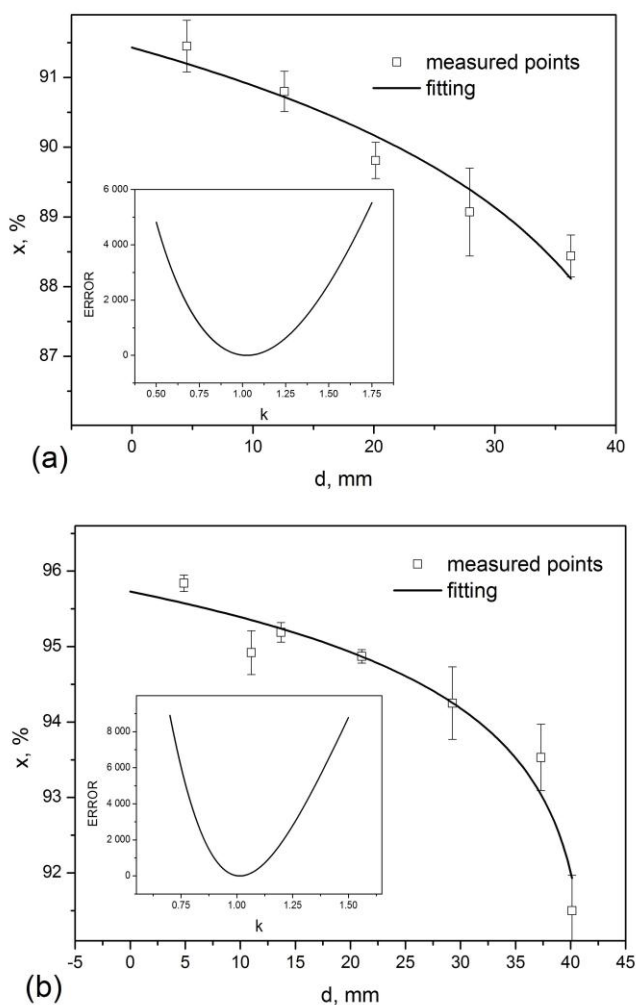


Fig. 3 The composition profiles along crystal rods for $\text{Cd}_{0.1}\text{Zn}_{0.9}\text{Te}$ (a) and $\text{Cd}_{0.04}\text{Zn}_{0.96}\text{Te}$ (b) compounds, points refer to experimental results and lines are best theoretical fits with least square method. An error arising from the fitting procedure is given in the inset.

It is known that every ternary alloy can be treated as mixture of two binary compounds. Under the condition of complete mixing of two binary semiconductors during the growth process one can assume that the controlling mechanism of compositional profile is convection in the melt. This is also the case of $\text{Cd}_{1-x}\text{Zn}_x\text{Te}$ mixed crystals [15]. Assuming thermal equilibrium state the composition along crystal rod is expected to follow monotonically the Pfann equation [15,16]:

$$x(d) = kx_0 \left(1 - \frac{d}{L}\right)^{k-1} \quad (1)$$

where: $x(d)$ is the composition changes as a function of distance d , k denotes a segregation coefficient, x_0 is an initial concentration and L is the total crystal rod length.

Fig. 3 presents composition variation along crystal rods for $\text{Cd}_{0.1}\text{Zn}_{0.9}\text{Te}$ (a) and $\text{Cd}_{0.04}\text{Zn}_{0.96}\text{Te}$ (b) compounds. Experimental points are values presented in Table 1 and error bars refer to the standard deviation. Lines are theoretical fittings of Eq. (1) using least square method with determination coefficients 0.9335 (a) and 0.9444 (b). The error of fitting is displayed in the insets of the graphs. It was assumed that minimum in the error curve corresponds to the segregation coefficient value which was found to be close to unity in both cases (1.025 and 1.013 for $\text{Cd}_{0.1}\text{Zn}_{0.9}\text{Te}$ and $\text{Cd}_{0.04}\text{Zn}_{0.96}\text{Te}$ alloy, respectively). Similar results of k_{Zn} value were obtained for all crystals presented in Table 1.

Segregation coefficient of zinc in CdTe matrix can vary within wide range from the lowest value 1.05 up to 1.6 [15]. The reason of this discrepancy is dependence of segregation coefficient on initial zinc concentration, applied thermal gradient profile, growth technique, pulling rate and rotation speed. The lowest value of k_{Zn} was obtained for crystals grown in vertical Bridgman with Accelerated Crucible Rotation Technique [15]. The crystals obtained within this work exhibit good both axial and radial homogeneity and as conclusion of this section one can say that applied vertical Bridgman technique is suitable for growing good quality homogenous crystals.

2.2 Experimental systems

PPE standard experimental setup described previously [11,17] for front and back measurement detection configuration was applied. In brief, it consisted of electronically modulated 300 mW power blue diode laser ($\lambda=405$ nm), a 0.4 mm thick LiTaO_3 detector ($\alpha_p=1.36 \times 10^{-6} \text{ m}^2 \cdot \text{s}^{-1}$ and $e_p=3660 \text{ W} \cdot \text{s}^{1/2} \cdot \text{m}^{-2} \cdot \text{K}^{-1}$ [18]), provided with CrAu electrodes and a SR850 dual-phase lock-in amplifier. In PPE method an optically opaque sample is placed onto the sensor. Exciting radiation impinges the sample or the sensor, depending on the measurement configuration. In case when laser excites directly the sample generated heat is travelling through the plate and is detected by the sensor. This is back configuration, since detector is placed from opposite side than excitation takes place. Back configuration returns information about thermal diffusivity of the sample. On the other hand, in front configuration laser radiation impinges the sensor and the sample acts like kind of heat sink. The measurement in this case gives thermal effusivity value of the specimen. In both configuration

to ensure good thermal contact between the sample and the sensor a thin layer of ethylene glycol was used as a coupling fluid ($\alpha_g=9.36 \times 10^{-8} \text{ m}^2 \cdot \text{s}^{-1}$ and $e_g= 814 \text{ W} \cdot \text{s}^{1/2} \cdot \text{m}^{-2} \cdot \text{K}^{-1}$ [18]). The modulation frequency of the excitation source was changed in the range 1 to 15 Hz and 5 to 45 Hz in case of back and front mode, respectively. For both BPPE and FPPE configuration normalization procedure with empty sensor was applied [11].

Transmission spectra were measured using standard UV-VIS spectrophotometer (Lambda2, PerkinElmer). All measurements presented in this work have been performed at room temperature and were computer-controlled.

3 Basic theory of PPE

The thermal diffusivity of the solid sample can be obtained with back PPE technique using so-called *phase-lag* method [11,12,19]. The expression describing the behaviour of the normalized phase Θ_n as a function of chopping frequency f is given by:

$$\Theta_n = \Theta_0 - L_s \left(\frac{\pi f}{\alpha_s} \right)^{1/2} \quad (2)$$

where: L_s and α_s are the thickness and thermal diffusivity of the sample, respectively.

Thermal diffusivity of the sample can be determined from the slope a of the phase graph as a function of the square root of the chopping frequency from simple formula [11]:

$$\alpha_s = \frac{L_s^2 \pi}{a^2} \quad (3)$$

In the front configuration one can measure thermal effusivity of the specimen. The expression for the normalized phase in this case is described by:

$$\Theta_n = \arctan \frac{(1 + R_{sp}) e^{-a_p L_p} \sin(a_p L_p)}{1 - (1 + R_{sp}) e^{-a_p L_p} \cos(a_p L_p)} \quad (4)$$

where: $R_{sp} = (b_{sp} - 1)/(b_{sp} + 1)$ is the reflection coefficient of the thermal wave at sample/pyro interface, $b_{sp} = e_s / e_p$ and e is the thermal effusivity, a_p is the reciprocal of the thermal diffusion length μ_p , $a_p = 1/\mu_p$, $\mu_p = (2\alpha_p/\omega)^{1/2}$, ω is the angular modulation frequency and L_p is the thickness of the sensor.

Both equation, (2) and (4), are valid under condition that thermal wave propagating through the sample and/or the sensor is attenuated at least e times on the distance equal to their thickness. Once this condition is satisfied one call it thermal thick regime or one can say the sample/sensor is thermally thick.

For phase normalized with empty sensor signal true is [11]:

$$\frac{L_p}{\mu_p} = \pi \Rightarrow \alpha_p = \frac{L_p^2 f_o}{\pi} \quad (5)$$

where f_o is frequency, when phase is crossing zero point and becomes negative. If the sample under examination is known, Eq. (5) allows determining thermal diffusivity of the used detector.

Thermal parameters are connected with each other. Thanks to that thermal conductivity k of the specimen can be calculated using following simple relation [11]:

$$k = e\alpha^{1/2} \quad (6)$$

4 Experimental results and discussion

4.1 Bowing parameter determination

Fig. 4 presents transmission spectra of $\text{Cd}_{1-x}\text{Zn}_x\text{Te}$ crystals for different composition. All samples were cut from the same position from crystal rod denoted Roman V (see Fig. 2). Since energy gaps of $\text{Cd}_{0.93}\text{Zn}_{0.07}\text{Te}$ and $\text{Cd}_{0.05}\text{Zn}_{0.95}\text{Te}$ alloys are very close to binary crystals CdTe and ZnTe, respectively, results obtained for given samples were omitted.

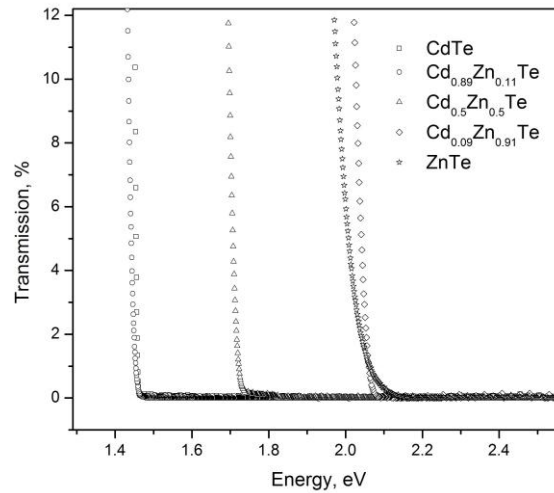


Fig. 4 Transmission spectra of $\text{Cd}_{1-x}\text{Zn}_x\text{Te}$ crystals for different composition.

Energy gaps were determined as the point where transmission approaches zero, however one should keep in mind that this is very roughly determined value. The real E_g of CdTe and ZnTe binary crystals was obtained by the author previously from photoluminescence and piezoelectric spectroscopy [20] with uncertainty of the order of 10 meV. Comparison study of earlier and present results lead to conclusion that the E_g read from transmission spectrum in this particular case is always underestimated about 50 meV. Observed discrepancy is mainly

due to two facts: (i) the thickness of the samples was about 1 mm and (ii) the dynamic of used spectrometer was only three orders in magnitude (max absorbance was 3).

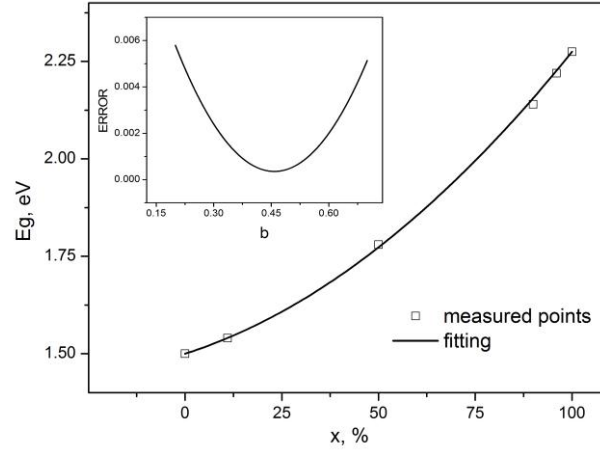


Fig. 5 Energy gap of the $\text{Cd}_{1-x}\text{Zn}_x\text{Te}$ crystals as a function of composition, squares are measured points, line is the best fit of Eq. (7) using least square method. Error arising from the fitting procedure is displayed in the inset.

It is well known that the variation of the band-gap energy with the composition for ternary alloys is described by the quadratic equation, which in case of $\text{Cd}_{1-x}\text{Zn}_x\text{Te}$ crystals can be assumed as:

$$E_{\text{Cd}_{1-x}\text{Zn}_x\text{Te}}(x) = xE_{\text{ZnTe}} + (1-x)E_{\text{CdTe}} - x(1-x)b \quad (7)$$

where: E_{ZnTe} and E_{CdTe} are the energy gaps for pure ZnTe and CdTe semiconductors, respectively, and b is the bowing parameter.

Obtained energy gap values of the $\text{Cd}_{1-x}\text{Zn}_x\text{Te}$ crystals as a function of composition are presented in Fig. 5. Squares are determined points and line is the best fit of Eq. (7) with the determination coefficient $R^2=0.999412$. The minimum in the error arising from the fitting procedure (see inset in Fig. 5) corresponds directly to the bowing parameter value b which was found to be 0.458. This value remains in general agreement with results obtained by other researchers. Reno and Jones [21] got very similar value (0.463) of the b parameter for ternary $\text{Cd}_{1-x}\text{Zn}_x\text{Te}$ alloys grown on GaAs substrate by MBE, however at 4 K. On the other hand, Samanta *et al* demonstrated bowing parameter value of $\text{Cd}_{1-x}\text{Zn}_x\text{Te}$ crystals at room temperature as 0.46 [22].

4.2 Experimental thermal results

Phase characteristics of $\text{Cd}_{1-x}\text{Zn}_x\text{Te}$ crystals for all zinc content measured in back configuration as a function of square root of modulation frequency are presented in Fig. 6. Since the thickness of the specimens varies from 1 to almost 1.6 mm the x data for every

sample was multiplied by its thickness. Thanks to that the difference in the slopes of obtained curves is directly proportional to the thermal diffusivity of given specimens.

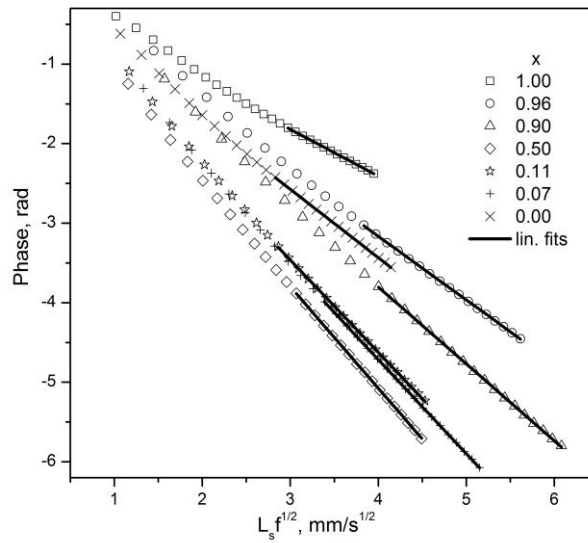


Fig. 6 Phase characteristics of $\text{Cd}_{1-x}\text{Zn}_x\text{Te}$ crystals for all zinc content measured in back configuration as a function of the square root of the modulation frequency multiplied by the thickness of the sample, points are experimental data and lines are linear fits obtained with least square method.

Linear fits were performed in the range of frequency where both, the sample and the sensor are thermally thick. The statistical determination coefficient R^2 describing quality of fitting was better than 0.9999 for all cases. One can see in Fig. 6 that the specimens with highest and lowest thermal diffusivity are ZnTe and $\text{Cd}_{0.5}\text{Zn}_{0.5}\text{Te}$, respectively. The thermal diffusivity of investigated specimens was calculated according to Eq. (3).

Fig. 7 (a) and (b) present measured phase in case of front configuration and example fit for $\text{Cd}_{0.5}\text{Zn}_{0.5}\text{Te}$ crystal, respectively. For clarity purposes the results for three selected crystals are only given. The fit of the theoretical curve to the experimental data was done with Eq. (4) applying least square method. The determination coefficient was of the order 0.999, slightly lower than in case of back configuration. The error of the fitting is given in the inset of the picture (b). The minimum observed in the error graph indicates sought thermal effusivity value of investigated sample. One can observe that all curves presented in Fig. 7 (a) cross the zero point more or less at the same modulation frequency. This observation supports the statement about proper measurement procedure.

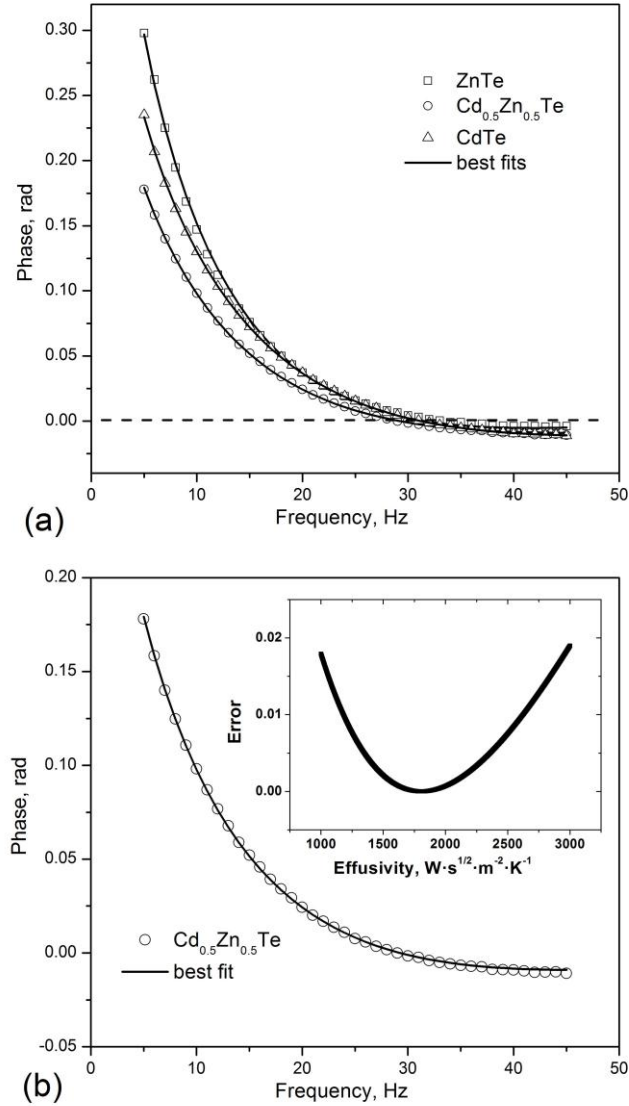


Fig. 7 Phase characteristics of selected $\text{Cd}_{1-x}\text{Zn}_x\text{Te}$ crystals as a function of modulation frequency (a), points refer to measured data, lines are best fits obtained with least square method using Eq. (4). Example fit for $\text{Cd}_{0.5}\text{Zn}_{0.5}\text{Te}$ crystal (b) and the error of the fitting procedure (see inset) is also shown.

4.3 Lattice thermal resistivity

Once the thermal diffusivity and effusivity are determined, one can calculate thermal conductivity of the specimens using Eq. (6). All thermal parameters and the thickness of the samples as the function of composition are given in Table 2. Thermal diffusivity and effusivity values were determined as average from three independent measurements with standard deviation as uncertainty. Whereas the error of thermal conductivity was estimated using total differential method. One can see in Table 2 that the uncertainties are of the order of 1% of measured value or even less proving good experimental repeatability. Another source of the error is the accuracy (0.01 mm) of used micrometer device for the thickness measurement, which produces 1-1.5% uncertainty. The most important and hard to estimate is the error connected with the presence of coupling fluid (ethylene glycol) between the sample

and the sensor. However, previously published work showed that this uncertainty can be minimized and is of the order 2-3% [23]. All contributions combined together give total uncertainty of obtained values of 4-5.5%.

Table 2 Thermal parameters and the thickness of the investigated Cd_{1-x}Zn_xTe crystals.

X	Thickness (mm)	Thermal diffusivity (m ² ·s ⁻¹)×10 ⁻⁶	Thermal effusivity (W·s ^{1/2} ·m ⁻² ·K ⁻¹)	Thermal conductivity (W·cm ⁻¹ ·K ⁻¹)×10 ²
0	1.07	4.254 ±0.021	2532.0±27.7	5.222±0.070
0.07	1.47	2.740±0.008	2038.3±13.7	3.374±0.027
0.11	1.17	2.337±0.013	1868.3±2.9	2.856±0.012
0.50	1.16	1.901±0.039	1794.0±10.8	2.473±0.040
0.90	1.57	3.368±0.025	2600.0±17.8	4.771±0.050
0.96	1.45	4.881±0.015	3301.7±29.3	7.294±0.045
1	1.02	9.071±0.043	4387.3±57.3	13.214±0.204

Looking back at the Table 2 one can conclude that all thermal parameters behave in similar way in the function of the composition. Two binary CdTe and ZnTe crystals are better conductor if comparing even with Cd_{0.93}Zn_{0.07}Te or Cd_{0.04}Zn_{0.96}Te mixed compounds. This is characteristic and expected behavior of the crystals, when leading role in the heat transport plays the lattice. In case of wide band-gap II-VI semiconductors one can assume only phonon transport, neglecting carriers contribution [24]. However, case of semiconductor alloys requires taking into account additional effect, which is the result of a random distribution of constituent atoms in sublattice sites. Adachi [13] showed that the thermal resistivity $W(x)$ for ternary A_xB_{1-x}C alloy can be described by simple expression:

$$W(x) = xW_{AC} + (1-x)W_{BC} + x(1-x)C_{A-B} \quad (8)$$

where: W_{AC} and W_{BC} are binary thermal resistivities and C_{A-B} is a contribution arising from the lattice disorder. Eq. (8) can be easily transferred into lattice thermal conductivity $K(x)$:

$$K(x) = \frac{1}{W(x)} = \frac{1}{xW_{AC} + (1-x)W_{BC} + x(1-x)C_{A-B}} \quad (9)$$

Lattice thermal conductivity versus composition for Cd_{1-x}Zn_xTe alloys is presented in Fig. 8. The points are values given in Table 2 and the line is theoretical fit of Eq. (9) using least square method. The determination coefficient was found to be 0.995758. One can notice in Fig. 8 that the curve describing thermal conductivity as the function of the composition has a minimum for x=0.5. The most significant changes are at the beginning and at the end of the curve, meanwhile in the middle there is plateau. Contribution to the thermal resistivity C_{Cd-Zn} connected with chemical disorder was determined from the fitting as 139 W⁻¹·cm·K. This value is similar to obtained previously in case of Zn_{1-x}Mg_xSe (C_{Zn-Mg} =116 W⁻¹·cm·K) crystals and even identical when compared with Zn_{1-x}Be_xSe (C_{Zn-Be} =139 W⁻¹·cm·K) alloys [11]. On the other hand, obtained results are 2-6 times larger than in case of typical III-V crystals [13].

However, the character of the change of the thermal conductivity is in principal the same in case of both classes of the semiconductors.

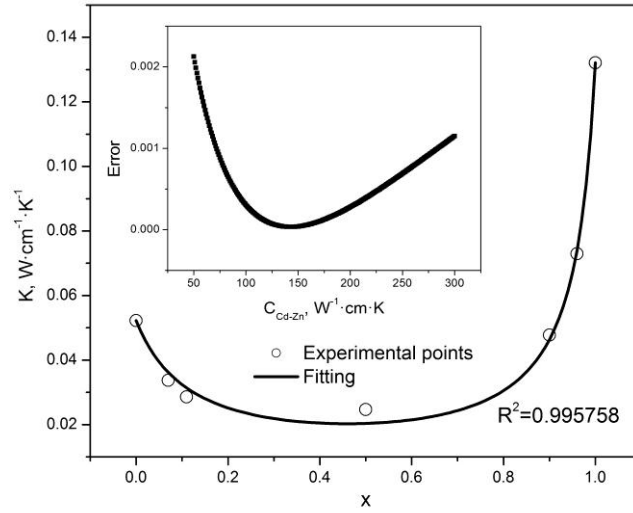


Fig. 8 Lattice thermal conductivity versus composition for $\text{Cd}_{1-x}\text{Zn}_x\text{Te}$ alloys (a). The points refer to the experimental data and solid line is best fit obtained using Eq. (9) with parameter $C_{\text{Cd-Zn}} = 139 \text{ W}^{-1} \cdot \text{cm} \cdot \text{K}$ applying least square method. Error arising from fitting procedure is shown in inset.

5 Conclusions

For the first time the systematical study of thermal properties of $\text{Cd}_{1-x}\text{Zn}_x\text{Te}$ alloys from one binary crystal (CdTe) to another (ZnTe) grown by vertical Bridgman technique were undertaken. The crystals were prepared for measurements in standard way. At the very first stage the composition was determined with SEM/EDS technique. The results showed both, radial and axial uniformity. Since the mechanism of the mixing was convection in the melt, the composition profiles followed the Pfann equation. The segregation coefficient for all $\text{Cd}_{1-x}\text{Zn}_x\text{Te}$ composition was found to be close to unity. The homogeneity of the crystal plates is of primary importance in case of potential application as x and gamma ray detectors. After the composition analysis standard transmission spectra were measured for all zinc content. Thanks to that energy gaps of investigated crystals as the function of composition were obtained. The variation of the band-gap energy with the composition was described by the quadratic equation, which allowed finding out the bowing parameter value equal 0.458. Obtained value remains in plausible agreement comparing with literature data. Thermal characterization of the $\text{Cd}_{1-x}\text{Zn}_x\text{Te}$ alloys has been performed using photopyroelectric technique applying both, back and front measurement configuration. Derived from the experiment thermal diffusivity and effusivity values allowed calculating thermal conductivity of the investigated semiconductors. Obtained results were analysed in the model given by Sadao Adachi for mixed ternary alloys. Contribution of the thermal resistivity arising from the lattice disorder to the total resistivity of the crystal has been determined as $C_{\text{Cd-Zn}} = 139 \text{ W}^{-1} \cdot \text{cm} \cdot \text{K}$.

References

- [1] T.E. Schlesinger, J.E. Toney, H. Yoon, E.Y. Lee, B. A. Brunett, L. Franks, R. B. James, *Mater. Sci. Eng. R* 32, 103 (2001).
- [2] H. Choi, *J. Korean Phys. Soc.* 66, 27 (2015).
- [3] C. Szeles, S. E. Cameron, J. O. Ndap, W. Chalmers, *IEEE Trans. Nucl. Sci.* 49, 2535 (2002).
- [4] S. Del Sordo, L. Abbene, E. Caroli, A. M. Mancini, A. Zappettini, P. Ubertini, *Sensors* 9, 3491 (2009).
- [5] A. Partovi, J. Millerd, E. M. Garmire, M. Ziari, W. H. Steier, S. B. Trivedi, M. B. Klein, *Appl. Phys. Lett.* 57, 846 (1990).
- [6] S. Sen, C. S. Liang, D. R. Rhiger, J. E. Stannard, H. F. Arlinghaus, *J. Electron. Mater.* 25, 1188 (1996).
- [7] C. Szeles, S. A. Soldner, S. Vydrin, J. Graves, D. S. Bale, *IEEE Trans. Nucl. Sci.* 55, 572 (2008).
- [8] C. Szeles, S. E. Cameron, S. A. Soldner, J. O. Ndap, M. D. Reed, *J. Electron. Mater.* 33, 742 (2004).
- [9] N. Zhang, A. Yeckel, A. Burger, Y. Cui, K. G. Lynn, J. J. Derby, *J. Cryst. Growth* 325, 10 (2011).
- [10] M. E. Rodriguez, J. J. Alvarado-Gil, I. Delgadillo, O. Zelaya, H. Vargas, F. Sanchez-Sinencio, M. Tufino-Velazquez and L. Banos, *Phys. Stat. Sol. A* 158, 67 (1996).
- [11] K. Strzałkowski, *Mater. Chem. Phys.* 163 (2015) 453.
- [12] D. Dadarlat, *Laser Phys.* 19 (2009) 1330.
- [13] S. Adachi, *J. Appl. Phys.* 54 (1983) 1844.
- [14] F. Firszt, S. Łęgowski, H. Meczynska, J. Szatkowski, W. Paszkowicz, K. Godwod, *J. Cryst. Growth* 184/185 (1998) 1335.
- [15] *Properties of Narrow Gap Cadmium based Compounds*, edited by P. Capper (INSPEC, IEE, London, UK, 1994) pp.501-503 and the references therein.
- [16] S. Miotkowska, E. Dynowska, I. Miotkowski, H. Alawadhi, A. Lewicki, P.A. Metcalf and A.K. Ramdas, *Acta Phys. Pol. A* 101 (2002) 735.
- [17] K. Strzałkowski, M. Streza, M. Pawlak, *Measurement* 64 (2015) 64.
- [18] D. Dadarlat, M. Streza, M.N. Pop, V. Tosa, S. Delenclos, S. Longuemart, A. Hadj Sahraoui, *J. Therm. Anal. Calorim.* 101 (2010) 397.
- [19] M. Chirtoc, G. Mihailescu, *Phys. Rev. B* 40 (1989) 9606.
- [20] K. Strzałkowski, J. Zakrzewski, M. Maliński, *Int. J. Thermophys.* 34 (2013) 691.
- [21] J. L. Reno and E. D. Jones, *Phys. Rev. B* 45 (1992)1440.
- [22] B. Samanta, S. L. Sharma, and A. K. Chauduri, *Vacuum* 46 (1995) 739.
- [23] K. Strzałkowski, D. Dadarlat, M. Streza, F. Firszt, *Thermochim. Acta* 614 (2015) 232.
- [24] G. Slack, *Phys. Rev. B* 6 (1972) 3791.